Controlling the Performance of Silicalite-1 Membranes

Leszek Gora,* Jacobus C. Jansen, and Thomas Maschmeyer*[a]

Abstract: The structural and performance characteristics (for *n*- and *i*-butane separation) of self-supported silicalite-1 membranes, were optimised by fine-tuning their syntheses by screening a total of nine silica sources and many reaction conditions. The mass balances indicate that membrane thickness is a function of both the synthesis volume and the silica source used. The excellent properties of the final membrane are demonstrated by its high permselectivity of 31 for *n*-butane combined with a *n*-butane flux of 10 mmol $m^{-2} s^{-1}$, indicating perfect performance. For 50/50 mixtures (of *n* and *i*) the selectivity for *n*-butane was 48 and its flux was 3.8 mmol $m^{-2} s^{-1}$. For the given selectivities, in relation to the membrane thickness, the theoretical fluxes are the highest values ever reported, underlining the point that high structural integrity is essential to achieve superior functionality.

Keywords: mass balance · membranes · separations · silicon · zeolites

Introduction

The interest in potential applications of zeolite membranes for separations at the molecular level is reflected in the rapid increase of studies dealing with their syntheses and testing.[1–15] These developments are of great technological importance as well as of great scientific interest. Well-defined, crystalline, hydrothermally stable membranes offer great versatility for many applications; their selectivity is determined by the reaction and separation processes employed. Ample scope exists for designing specific membranes to generate tailor-made systems. However, some practical hurdles still need to be overcome, and further fundamental insight needs to be gained before the development of such membrane systems is routine. Zeolite membranes are most commonly prepared by single- or multistep, in situ hydrothermal crystallisation on a flat or tubular porous support at 100 – 180 °C, either from a solution or a gel of aluminosilicate. Methods involving secondary growth on seeded supports for zeolite membrane processing[1, 2] as well as vapor-phase deposition[3] have been introduced recently. Zeolite membranes, mostly MFI type, can be grown on porous supports such as stainless steel,[4–6] anodic alumina,[7] α-alumina,[6, 8a, 9–11] γ-alumina,[9b, 12] clay composites,[5a] glass,[13] and carbon with a $ZrO_2 - TiO_2$ coating.[14] Depending on the experimental conditions, the thickness of the zeolite membrane can be varied from a few hundred[6] to a few micrometers.[8] On most porous supports the zeolite layers are firmly bonded through surface hydroxy groups, whereas non-porous teflon, as an inert support, is easily separated from a zeolite layer. The syntheses of self-supported MFI membranes prepared by removal from teflon slabs were first reported by Sano et al.[16] and Tsikoyiannis et al.[17] Another method involves the synthesis of MFI membranes on cellulose filter paper, in which the self-supported zeolite layers are formed by burning off the cellulose phase.[18] A mercury surface was also used as a substrate for the growth of a self-supported film of MFI type zeolite.[19] Although, the supported zeolite membrane has better mechanical properties than a self-supported zeolite layer, the macropores of the support affect the membrane performance as reported by van de Graaf et al.[20] A support can significantly influence the concentrations of permeates at the interface of the support/zeolite layer, reducing the selectivity and the flux. For fundamental studies, the self-supported zeolite layer should reveal the most representative behaviour of zeolite membranes; however, owing to mechanical constrictions a thickness of at least 50 μm is unavoidable.

In this study, we have explored the influence of different types of silica sources and aging effects on zeolite layer formation. Both the mass balance as well as the variation in thickness of the unsupported zeolite layers due to changes in the volume of the reaction mixture were determined. Finally, the gas permeability of the resulting films were measured.

[a] Dr. L. Gora, Prof. T. Maschmeyer, Assoc. Prof. J. C. Jansen
Laboratory for Applied Organic Chemistry and Catalysis,
DelftChemTech, Delft University of Technology
Julianalaan 136, 2628 BL, Delft (The Netherlands)
Fax: (+31) 15-278-4289
E-mail: L.Gora@tnw.tudelft.nl

Experimental Section

Film preparation: The molar ratio of the synthesis mixture was: 100 SiO_2:123 tetrapropylammonium (TPA):63.7 OH:14 200 H_2O. The zeolite synthesis solution was prepared by mixing tetrapropylammonium

  0947-6539/00/0614-2537 $ 17.50+.50/0

hydroxide (Chemische Fabriek Zaltbommel CFZ B.V., 25% in water), tetrapropylammonium bromide (CFZ B.V.) and dionized water. After TPABr was dissolved completely, one of the following silica sources was added to the solution: Aerosil 200 (Degussa), Aerosil OX50 (Degussa), TEOS (Merck), silica gel 40 (Fluka), silica gel Davisil 646 (Aldrich), colloidal silica 30% (Aldrich), Ludox AS-40 (DuPont), Ludox LS (DuPont) or Ludox HS-40 (DuPont). The synthesis mixture was aged and stirred at room temperature until the solution became clear. Comparable experiments without aging were also performed.

A teflon disk (35 mm in diameter) was placed in a 55-mL teflon-lined autoclave to which the reaction mixture was added. The autoclaves were placed in a hot air oven at either 180 °C for 17 h or 140 °C for 67 h. After the autocalve had been allowed to cool, the teflon disk was removed, washed and dried. The film was removed from the teflon using a small spatula. It was possible to remove most samples (see Figure 1) without disintegration, but with others it was more difficult, the layer thickness and phase continuity of the membranes having a strong effect. The films were than calcined for 16 h in air at 400 °C with a heating and cooling rate of 1 K min^{-1}, respectively. The mass of product on the disk, on the wall of the autoclave and from solution were determined systematically.

Characterisation: An optical microscope, Olympus BH2, was used for estimating the membrane integrity and the presence of cracks in the layer before and after calcination. Both sides of the layer as well as the thickness (cross section) were examined by scanning electron microscopy (SEM) using a Philips XL20 microscope. X-ray diffraction analysis was carried out on the zeolite disk using a Philips PW 1830 X-ray diffractometer.

Permeation: Measurements were performed at 298 K for the single gases *n*-butane and *i*-butane as well as for 1:1 mixtures (50 kPa of each gas). A piece of zeolitic film was glued with epoxy resin onto a flange, which had a 0.25 cm^2 window. The flange was placed in a Wicke – Kallenbach cell and the permeability was measured by mass spectrometry.[5] The feed side was at a pressure of 101 kPa. At the permeate side pure helium as a sweep gas was used at a flow of 100 mL min^{-1}, keeping the pressure difference over the membrane at zero. Both sides of the membrane were analysed for gas composition, covering transient and steady-state scenarios. The membrane flux was directly calculated from the gas flow rates and the compositions of the permeate and of the retentate.

Calculations of the minimised energy positions of the *n*- and *i*-butane molecules in the double 10-ring of silicalite-1 were carried out with the Cerius2 suite of programs; *n*- and *i*-butane were built using the 3D-sketcher, with atomic charges from MOPAC. The Dreiding 2.21 force field was applied for the calculations. The Smart Minimiser was used to minimise the energy of the hydrocarbons in vacuum and in the zeolite. Minimisation was terminated if the RMS force dropped below 0.1 kcal mol^{-1}.

Table 1. Silica sources used and precursors arranged according to the zeolite films.

Silica source		Precursor	Zeolite crystal film
TEOS	Merck	monomeric	perfectly intergrown (see Figure 1)
fumed silica Aerosil 200 Aerosil OX50	Degussa	segregated gel from primary particles	multilayer of well-connected crystallites (see Figures 2 and 3)
gel silica Davisil 646 40	Aldrich Fluka	segregated gel from gel bodies	multilayer of poorly connected crystallites (see Figure 2a – f)
colloidal silica no spec. Ludox AS-40 LS HS-40	Aldrich Du Pont		

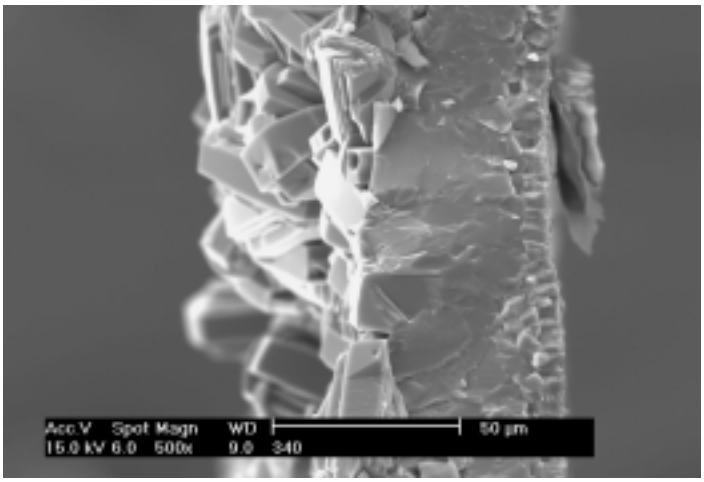

Figure 1. Cross section of unsupported silicalite-1 layer synthesised at 180 °C. TEOS as a silica source. Solution aged 6 h.

Results and Discussion

Effect of silica sources and aging on the membrane formation

In Table 1 the various silica sources used are arranged on the basis of the zeolite films formed. With TEOS as a silica source the layer of 50 µm has a perfectly intergrown appearance according to SEM observations of a cross section (Figure 1). Transmission electron microscopy (TEM) measurements did not reveal pinholes in the nanometer range. The membrane synthesis under the optimal conditions described in this study gives membranes with a high selectivity, equal to 48 and a flux of 3.8 mmol m^{-2} s^{-1} (Table 2). As the precursor phase is monomeric silica, after hydrolysis/aging (Table 1) the membrane phase is nucleating and growing from a homogeneous synthesis solution, resulting in a perfectly intergrown layer, and is close to a microporous continuous phase. Fumed silica particles on the other hand form gel particles that segregate.[21] As the synthesis mixture is not stirred, the highly supersaturated solution at the bottom of the autoclave is in equilibrium with the silica/gel phase covering the support. It can be concluded from in situ observation that nucleation starts at the interphase of the gel particles and the solution.[21] Preferred growth occurs in the direction of the highest silica concentrations (i.e. the gel phase), and only slowly do the individual crystals grow together. Finally, crystal growth results in an almost closed membrane of clearly observable crystals, but a perfectly intergrown layer (such as that shown in Figure 1) is not formed. When the gel phase is consumed by the crystal growth, pinholes might remain between the crystals as the density of the gel (1.4 g cm^{-3}) is smaller than the density of the crystals (1.99 g cm^{-3}).[21] Triangular pinholes are present in a regular arrangement,[22] thereby reducing the performance of the zeolite membrane. In the last group of silica sources silica gel or colloidal silica is used. The segregated precursor phase, comprising larger particles or more chemically resistant particles, converts upon increasing the temperature into an even less closed crystal layer. Individual crystals, although grown together, are easily observed (Figures 2a – f). The main transport can be described as Knudsen diffusion and viscous flow.

0947-6539/00/0614-2538 $ 17.50+.50/0 *Chem. Eur. J.* **2000**, *6*, No. 14

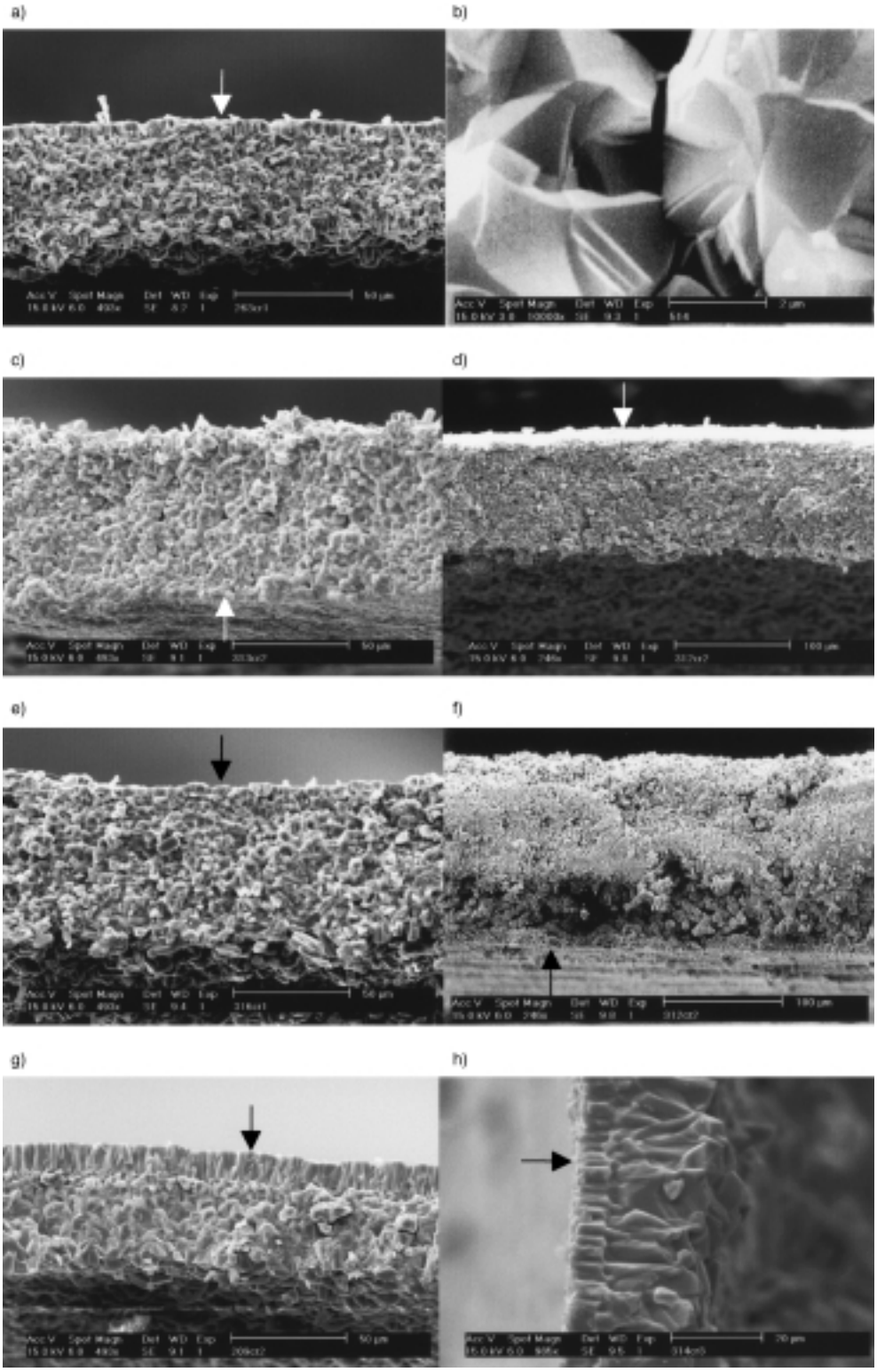

Figure 2. Cross sections of unsupported silicalite-1 layers synthesised at 140 °C. Different silica sources, solution aged 6 h prior to synthesis; a) silica gel Davisil, b) enlargement of (a), c) silica colloidal 30 % SiO_2, d) Ludox LS, e) Ludox AS-40, f) Ludox HS-40, g) Aerosil 200, h) TEOS. Arrows show the surface that was in contact with the teflon during synthesis.

Figures 2a–h show cross sections of layers synthesised at 140 °C with an aged reaction mixture using different silica sources. Irrespective of the type of silica sources used, the zeolite films show a double layer of crystals. The ratio of the thickness between the two layers depends on the type of silica. The first layer, bordering the teflon slab, is hardly observed in samples prepared with colloidal silica, whereas it is clearly visible in samples made with fumed silica or with TEOS. Apparently in the course of the synthesis, crystal growth from the support is covered by aggregates of the precursor and subsequently by crystals. In the case of colloidal silica, the precipitation from solution is dominant from the start and

  0947-6539/00/0614-2539 $ 17.50+.50/0

Table 2. Comparisons of *n*-butane fluxes and ideal n-C_4H_{10}/i-C_4H_{10} permselectivity and selectivity through zeolite membranes at room temperature by usiing the Wicke – Kallenbach method. The permeate pressure was kept at 101 kPa.

Zeolite/support	δ [μm]	Flux [mmol m^{-2}s^{-1}]	Selectivity	*n*-butane fluxes corrected for the membrane thickness [10^{-6}mmol m^{-1}s^{-1}]	Ref.
Single component (101 kPa)					
ZSM-5/α-Al_2O_3	10	0.95[a]	18.4	9.5	[9a]
silicalite-1/γ-alumina	5	5.9[a]	20	29.5	[29]
silicalite-1/α-Al_2O_3	<5	0.67 – 3.8	48 – 131	19	[8]
silicalite-1/stainless steel	50	4.2	58	210	[4]
ZSM-5/α-Al_2O_3	10	0.4	32	4	[9b]
ZSM-5/α-Al_2O_3	10	0.25	322[c]	2.5	[9c]
silicalite-1/α-Al_2O_3	[b]	1.2	56	–	[30]
ZSM-5/α-Al_2O_3	20	1.6	10	32	[31]
unsupported silicalite-1	50	10	31	500	this work
1:1 mixture (50 kPa:50 kPa)					
silicalite-1/α-Al_2O_3	<5	0.83	52	4.2	[8a]
silicalite-1/Stainless steel	50	2.2	21	110.0	[32]
silicalite-1/Stainless steel	50	1.5	27	75.0	[4]
silicalite-1/α-Al_2O_3	>5	1.3	52	6.5	[8b]
silicalite-1/α-Al_2O_3	15	4.86[d] $\pm$ 0.84	38.4 $\pm$ 14	72.9	[2]
silicalite-1/α-Al_2O_3	30	1.99[e] $\pm$ 0.5	50.75 $\pm$ 11	60.0	[2]
unsupported silicalite-1	50	3.78	48	189.0	this work

[a] Results obtained from permeation $J = \Delta p$. [b] No data available. [c] Data obtained at 105 °C. [d] Average from two membranes. [e] Average from six membranes.

Table 3. Thickness of unsupported silicalite-1 layers in μm. Synthesis solutions, aged (+) or not aged (−).

Silica source	140 °C and 67 h.		180 °C and 17 h.	
	+	−	+	−
Aerosil 200	50 – 60	50	50 – 70	60 – 100
Aerosil OX50	50	50	50	50
TEOS	28	–	50	–
silica gel 40	75 – 100	–	100	–
silica gel Davisil	55	–	50 – 65	–
silica colloidal, 30 %	65 – 85	125		
Ludox AS-40	70 – 90	75		
Ludox LS	110	120		
Ludox HS-40	150 – 200	150 – 175		

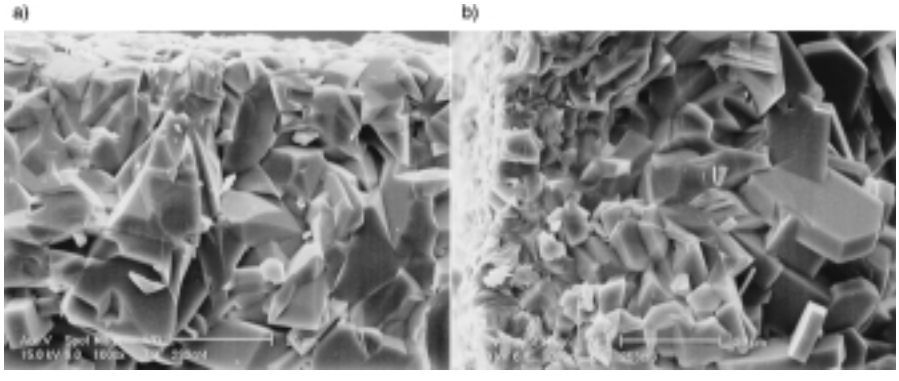

Figure 3. Cross section of unsupported silicalite-1 layer synthesised at 180 °C. Aerosil 200 as a silica source; a) solution not aged, b) solution aged 6 h.

growth from the support is hardly developed. X-ray diffraction (XRD) analyses showed that all samples were fully crystalline. Preferential orientation was not observed. The total thickness of the layers varies from 28 μm to 200 μm depending on the silica source. A relatively thin film can be synthesised with TEOS compared to the thick films made with Ludox HS-40. Most probably the supply of nutrient/mass induced by gravity forces is higher in the case of aggregated silica particles, from for example HS-40, than in the case of molecularly dissolved TEOS. Based on the above data, silicalite-1 membranes prepared with TEOS are the best regarding the continuity of the zeolite phase.

The increase of the nucleation and crystal growth rate upon aging of the reaction mixture, in particular for low Si/Al systems, has been well-studied.[23] In the cases of aging of all-silica mixtures, the silica phase might either dissolve or reorganise in the gel, depending upon the type of silica source. Table 3 shows that when TEOS or silica gels were used it was necessary to age the reaction mixture in order to grow silicalite-1 films. Figures 3a and 3b depict cross sections of layers synthesised with and without aging, respectively, at 180 °C with Aerosil 200. The film synthesised from the non-aged mixture is formed by relatively large crystals (Figure 3a), while in the layer crystallised from the aged mixture the crystals are smaller. In both cases the layer has a comparable thickness, and the crystal size decreases gradually from the top to the bottom of the layer (Table 4). The crystal size decreases 18 % upon aging, prior to the synthesis at 140 °C, while at 180 °C, this decrease is at least 70 %. An advantage of small crystals obtained by aging is that the thickness of the membrane as well as the size of pinholes can be reduced.

Mass balance determination and layer thickness

Figure 4 shows the linear correlation between the total mass of silicalite-1 formed in the reactor and the volume of the synthesis mixture. Pertaining to the mass of silica in solution and the mass of silica in the total product, the yield of the synthesis is about 52 % in the case of TEOS as Si-source (at 180 °C and 17 h). Figure 5a indicates that the mass of the zeolite layer expressed in the layer thickness is extremely small below a synthesis volume of 5 mL. Almost no crystals are observed on the teflon support. This 'hold up' volume is present between the disk and the walls, the bottom of the autoclave and partly

0947-6539/00/0614-2540 $ 17.50+.50/0 *Chem. Eur. J.* **2000**, *6*, No. 14

Table 4. Crystal sizes[a] in the silicalite-1 layer [μm].

	Solution aged [h]	Reaction temperature 140 °C	180 °C
0	top view	20–15	70–20
	bottom side	6–5	20–18
6	top view	16–10	25–14
	bottom side	5–4	8–4

[a] Measured from SEM pictures.

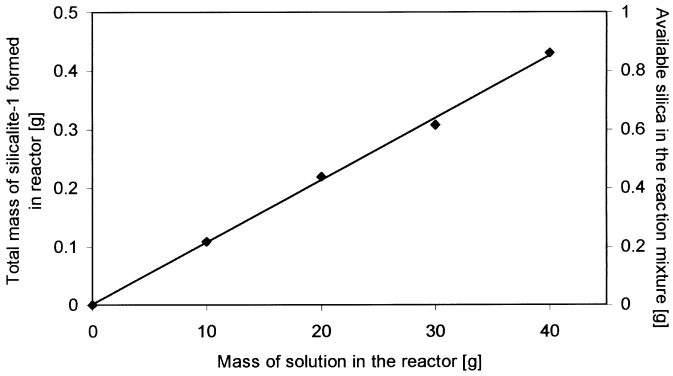

Figure 4. Plot of the total mass of silicalite-1 formed versus the amount of the reaction mixture in the reactor (TEOS, 180 °C).

on top of the disk. This volume contributes negligibly to the formation of the layer on the top of the disk. At a synthesis volume of 10 mL, of which only 5 mL is therefore a source to provide the mass for the layer, the zeolite layer thickness is 50 μm. The silica mass in this layer is then related to almost 100 % of the silica mass in the synthesis mixture available for this layer. The conclusion is that the mixture and synthesis conditions need to be well-balanced to obtain a high efficiency with regard to the formation of a layer. However, as indicated in Figure 5a, at 20, 30 and 40 g reaction mixtures the layer thickness remains unaltered. The residual crystal mass is recovered from the autoclave wall and the solution. Thus, the larger the mass, the larger the resulting competitive crystallisations; thus, the resulting layer thickness is more or less constant. Most probably there is no segregation of precursor species from the clear solution. Crystals formed from the solution deposit, but do not grow as a fixed phase on the 50 μm layer and are, hence, removed in the washing step.

Figure 5b indicates that at lower temperature, even when employing longer synthesis times, 140 °C is too low to obtain

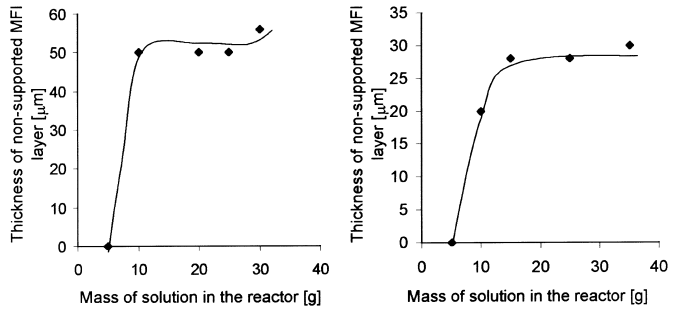

Figure 5. Plot of the thicknesses of non-supported silicalite-1 layers versus the amounts of reaction mixture in the reactor; a) TEOS, 140 °C, b) TEOS, 180 °C.

complete crystallisation from solution on the support. The layer thickness is maximal 30 μm. A comparable 'plateau', which is, however, smaller and lower is present in Figure 5b, indicating that apparently the same phenomenon occurs as in the experiment at 180 °C. In the case of Aerosil 200, at 180 °C and 17 h, the thickness of the layer is smaller and gradually grows upon using larger synthesis volumes. The efficiency of the synthesis is somewhat lower (about 48 %) which, however, cannot explain the final thinner layer formed. The difference in the layer thickness between Aerosil and TEOS is mainly caused by the sol particles of the Aerosil compared to those of TEOS, which induce a higher nucleation and crystallisation rate in the solution. The larger mass of crystals formed in solution compared to those formed in the TEOS experiment, is not available to contribute to the layer in the case of Aerosil. At the same time precursor species are aggregating in the case of Aerosil, thus, larger masses increase the layer thickness in contrast to the case for TEOS.

Reproducibility

An example of the reproducibility is shown in Table 5. Layers were prepared under the same conditions, that is Aerosil 200, ageing 6 h, 140 °C. The total mass of the zeolite layer and

Table 5. Reproducibility of the preparations of non-supported MFI layers, aerosil 200, 140 °C, 67 h, aged 6 h prior to synthesis.

No.	Mass of zeolite [g]	Total thickness of the layer [μm]	Thickness of the first layer facing Teflon [μm]
209	0.2971	60	13
210	0.2355	50	7
211	0.2882	60	14
212	0.3529	50	11
213	0.3207	50	10
226	0.3233	60	8
302	0.3359	50	9

crystals suspended in the bulk solution for six out of seven samples varied by less than 3.3 % from the average value. Layer thicknesses were very similar (between 50–60 μm). These results clearly show that the formation of silicalite-1 layers is reproducible under the conditions chosen. It is well established that during the first step of membrane crystallisation, the support is covered by a gel phase.[24] This gel phase is a precursor in the crystallisation. Formation of a gel layer covering the support as well as the nucleation of crystals can be controlled by adjusting the pH of the reaction mixture,[25] the concentration of SiO_2[25] and the temperature and heating rates during the induction period.[25, 26]

Permeation

The selectivity and fluxes of n-C_4H_{10}/i-C_4H_{10} are frequently used as an indication for the quality of the membrane. Permeation and selectivity measurements were conducted with films synthesised at 180 °C with TEOS as a silica source (see Figure 1). With the minimum kinetic diameter of 0.50 nm for i-butane, and of 0.43 nm for n-butane[27], both molecules can permeate through the silicalite-1 channel apertures (ca.

0.52×0.58 nm in the monoclinic phase[28]), and, therefore, no absolute separation, but separation based on configurational diffusion is envisaged. The *n*-butane flux was 10 mmol $m^{-2} s^{-1}$ and the permselectivity of *n*-butane to *i*-butane was equal to 31 (Table 1). As the experiments were carried out at 298 K, the permeation was principally based on surface diffusion of the molecules. As the surface of the pores is made up of siloxane linkages, the number and distance of the interactions with the alkanes is of the C–H ··· O van der Waals type. The different energies of diffusion are related to the interaction of the *n*- and *i*-butane molecules, characterised by their kinetic diameters, with the double 10-rings of silicalite-1, characterised by their apertures. As shown in Figure 6, a number of relatively short contacts is observed for *i*-butane compared to *n*-butane in the double 10-ring. Therefore, *n*-butane transport is higher than that of *i*-butane.

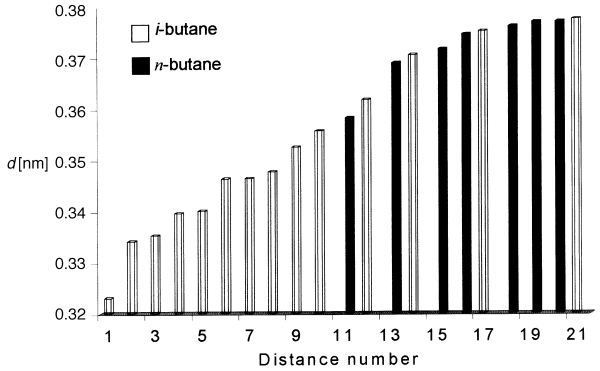

Figure 6. Distances *d* up to 0.38 nm from the minimised positions of the C atoms of *n*-butane and isobutane to the oxygen atoms of a double 10-ring in the sinusoidal channel of the monoclinic silicalite-1. The differences, in particular, of the shortest 'contacts' are substantial and indicative of the different degree of interaction and, hence, separation.

A more quantitative approach is an estimate of the highest separation versus flux. However, as there are no data in literature for unsupported membranes this is only possible for supported zeolite membranes (see Table 2 for details).[2, 4, 8, 9, 12, 14, 29–32] The data from the unsupported membrane indicate an almost perfect micropore phase in the case of single gas as well as mixed gas feeds; in particular, when the thickness is taken into account. The highest *n*-butane/*i*-butane ideal selectivity reported, thus far, is equal to 322[9c], using a ZSM-5/Al_2O_3 membrane modified by post-synthetic treatment, that is by triisopropylbenzene (kinetic diameter 0.84 nm) upon coking. Although this effectively closed macro/mesopores and defects of micropores present in the membrane, the improved selectivity is achieved at the cost of a very significant decrease in flux. While maintaining a very high selectivity, the flux of *n*-butane through the self-supported silicalite-1 film presented in this work is much higher than any other reported in the literature when the layer thickness is taken into account.

Acknowledgement

We are indebted to Ir. J. ter Horst of the Department of Apparatus for the Process Industry, Delft University, for the energy-minimisation calculations. This study was funded by NWO (Dutch Organisation for Science and Research).

[1] M. C. Lovallo, M. Tsapatsis, *AIChE J.***1996**, *42*, 3020 – 3029.
[2] G. Xomeritakis, A. Gouzinis, S. Nair, T. Okubo, M. He, R. M.Overney, M. Tsapatsis, *Chem. Eng. Sci.* **1999**, *54*, 3521 – 3531.
[3] E. Kikuchi, K. Yamashita, S. Hiromoto, K. Ueyama, M. Matsukata, *Microporous Mater.* **1997**, *11*, 107 – 116.
[4] W. J. W. Bakker, F. Kapteijn, J. Poppe, J. A. Moulijn, *J. Membr. Sci.* **1996**, *11*, 57 – 78.
[5] a) E. R. Geus, M. J. den Exter, H. van Bekkum, *J. Chem. Soc. Faraday Trans.* **1992**, *88*, 3101 – 3109;b) E. R. Geus, H. van Bekkum, W. J. W. Bakker, J. A. Moulijn, *Microporous Mater.* **1993**, *1*, 131 – 147.
[6] T. Sano, M. Hasegawa, Y. Kawakami, Y. Kiyozumi, H. Yanagishita, D. Kitamoto in *Zeolites and related microporous materials: State of the art 1994*, *Studies in surface and catalysis*, *Vol. 84* (Eds.:J. Weitkamp, H. G. Karge, H. Pfeifer,W. Holderich), Elsevier, **1994**, pp. 1175 – 1182.
[7] a) Y. H. Chiou, T. G. Tsai, S. L. Sung, H. C. Shih, C. N. Wu, K. J. Chao, *J. Chem. Soc. Faraday Trans.* **1996**, *92*, 1061 – 1066; b) Y. H. Chiou, T. G. Tsai, H. C. Shih, C. N. Wu, K. J. Chao, *J. Mater. Sci. Lett.* **1996**, *15*, 952 – 954.
[8] a) Z. A. E. P. Vroon, K. Keizer, M. J. Gilde, H. Verweij, A. J. Burggraaf, *J. Membr. Sci.* **1996**, *113*, 293; b) Z. A. E. P.Vroon, K. Keizer, A. J. Brggraaf, H. Verweij, *J. Membr. Sci.* **1998**, *144*, 65 – 76.
[9] a) Y. Yan, M. E. Davis, G. R.Gavalas, *Ind. Eng. Chem. Res.* **1995**, *34*, 1652 – 1661; b) Y. Yan, M. Davis, G. R. Gavalas, *J. Membr. Sci.* **1997**, *126*, 53 – 65; c) Y. Yan, M. Davis, G. R. Gavalas, *J. Membr. Sci.* **1997**, *123*, 95 – 103.
[10] K. Kusakabe,T. Kuroda,A. Murata,S. Morooka,*Ind. Eng. Chem. Res.* **1997**, *36*, 649 – 655.
[11] J. Coronas, R. D. Noble, J. L. Falconer, *Ind. Eng. Chem. Res.* **1998**, 37, 166 – 176.
[12] A. Giroir-Fendler, J. Peureux, H. Mozzanega, J-A. Dalmon in *11th International congress on catalysis-40th Anniversary*, *Studies in surface and catalysis*, *Vol. 101* (Eds.: J. W. Hightower, W. N. Delgass, A. T. Bell), Elsevier, **1996**, pp. 127 – 136.
[13] A. Ishikawa, T. H. Chiang, F. Toda, *J. Chem. Soc. Chem. Commun.* **1989**, *12*, 764 – 765.
[14] J. J. Jafar, P. M. Budd, *Microporous Mater.* **1997**, *12*, 305 – 311.
[15] M. J. den Exter, J. C. Jansen, J. M. van de Graaf, F. Kapteijn, J. A. Moulijn, H. van Bekkum in *Recent advances and new horizonts in zeolite science and technology*, *Taejon*, *Studies in surface science and catalysis*, *Vol. 102* (Eds.: H. Chon, S. I. Woo, S.-E. Park), Elsevier, **1996**, pp. 413 – 454.
[16] a) T. Sano, Y. Kiyozumi, M. Kawamura, F. Mizukami, H. Takaya, T. Mouri, W. Inaoka, Y. Toida, M. Watanabe, K. Toyoda, *Zeolites* **1991**, *11*, 842 – 845;b) T. Sano, Y. Kiyozumi, F. Mizukami, H. Takaya, T. Mouri, M. Watanabe, *Zeolites* **1992**, 12, 131 – 134.
[17] J. G. Tsikoyiannis, W. O. Haag, *Zeolites* **1992**, *12*, 126 – 130.
[18] T. Sano, Y. Kiyozumi, K. Maeda, M. Toba, S. Niwa, F. Mizumi in *Proceedings of the 9th International Zeolite Conference* (Ed.: R. von Ballmoos), Montreal, **1992**, pp. 239 – 246.
[19] Y. Kiyozumi, F. Mizukami, K. Maeda, T. Kodzasa, M. Toba, S. Niwa in *Progress in zeolite and microporous materials*, *Seoul*, *Studies in surface science and catalysis Vol.105* (Eds.: H. Chon, S.-K. Ihm, Y. S. Uh), Elsevier, **1997**, pp. 2225 – 2232.
[20] J. M. van de Graaf, F. Kapteijn, J. A. Moulijn, *J. Membr. Sci.* **1998**, *14*, 87 – 104.
[21] J. H. Koegler, H. van Bekkum, J. C. Jansen, *Zeolite* **1997**, *19*, 262 – 269.
[22] L. Gora, J. C. Jansen, T. Mashmeyer in *Porous Materials in Environmental Friendly Processes*, *Studies in Surface Science and Catalysis*, *Vol. 125* (Eds.: I. Kiricsi, G. Pal-Borbely, J. B. Nagy, H. G. Karge), Elsevier, **1999**, pp. 173 – 180.
[23] L. Gora, K. Streletzky, R. W. Thompson, G. D. J. Phillies, *Zeolites* **1997**, *18*, 119 – 131.
[24] J. C. Jansen, G. M. van Rosmalen, *J. Cryst. Growth* **1993**, *128*, 1150 – 1156.
[25] B. J. Schoeman, A. Erdem-Senatalar, J.Hedlund, J. Sterte, *Zeolites* **1997**, *19*, 21 – 28.
[26] J. H. Koegler, A. Arafat, H. van Bekkum, J. C. Jansen in *Progress in zeolite and microporous materials*, *Seoul*, *Studies in surface science and catalysis*, *Vol. 105* (Eds.: H. Chon, S. K. Ihm, Y. S. Uh), Elsevier, **1997**, pp. 2163 – 2170.
[27] D. W. Breck, *Zeolite Molecular Sieves*, Wiley, NY, **1974**, pp. 633 – 641.

  0947-6539/00/0614-2542 $ 17.50+.50/0

[28] H. van Koningsveld, J. C. Jansen, H. van Bekkum, *Zeolites* **1990**, *10*, 235–242.
[29] C. Bai, M.-D. Jia, J. L. Falconer, R. D. Noble, *J. Mater. Sci.* **1995**, *105*, 79–87.
[30] H. Moueddeb, P. Ciavarella, H. Mozzanega, S. Miachon, J.-A. Dalmon in *Proceedings of the Fifth International Conference on Inorganic Membranes*, Nagoya, June 22–26, **1998**, pp. 576–579.
[31] K. Kusakabe, S. Yoneshige, A. Murata, S. Morooka, *J. Mater. Sci.* **1996**, *116*, 39–46.
[32] J. M. van de Graaf, E. van der Bijl, A. Stol, F. Kapteijn, J. A. Moulijn, *Ind. Eng. Chem. Res.* **1998**, *37*, 4071–4083.

Received: September 27, 1999 [F2058]